Construction and Building Materials 71 (2014) 132–140

Contents lists available at ScienceDirect

Construction and Building Materials

journal homepage: www.elsevier.com/locate/conbuildmat

Evaluation of alkali–silica reaction in concretes with natural rice husk ash using optical microscopy

R. Zerbino [a,c,*], G. Giaccio [a,c], S. Marfil [b]

[a] Civil Eng. Department – UNLP, La Plata, Argentina
[b] CIC – Geology Department – UNS, Bahía Blanca, Argentina
[c] LEMIT, 52 entre 121 y 122, 1900 La Plata, Argentina

HIGHLIGHTS

- Alkali–silica reaction in concretes with natural RHA was studied.
- Concretes with RHA, under field conditions, were evaluated up to four years.
- Microscopy observations were done to identify reaction products and internal damage.
- In presence of alkalis RHA produces severe damage in concrete, but no gel was found.

ARTICLE INFO

Article history:
Received 8 October 2013
Received in revised form 6 August 2014
Accepted 23 August 2014
Available online 16 September 2014

Keywords:
Cement
Concrete
Mechanical properties
Microscopy
Rice-husk ash

ABSTRACT

The use of rice husk ash as a supplementary cementing material is of great interest to many developing countries where rice production is in abundance. A highly reactive pozzolan is obtained when rice husk ash is burnt under controlled conditions. Previous work showed that it is possible to use residual rice husk ash "as nature" (natural rice husk ash). Nevertheless, it was observed that the incorporation of natural rice husk ash implies risks of expansions and mechanical degradation due to the reactions with alkalis. Based on the performance of slab prototypes placed outdoors during more than 3 years, this work analyzes the causes and the damage processes involved in the development of expansions in presence of natural rice husk ash. Optical microscopy observations on thin sections; crack patterns of the slabs and the strength and surface strain evolution along the time were evaluated. Visual and microscope observations showed clear signs of damage due to expansive reactions in concretes incorporating natural rice husk ash when high alkalis contents are available; although not gel was found, numerous cracks and voids were observed close to unburned rice husk particles, as well as high expansions and significant decreases in strength and stiffness. In concretes with alkalis contents lower than 3 kg/m^3, even with the same percentages of natural rice husk ash, there were no significant decreases in the mechanical properties.

1. Introduction

Rice husk, an agricultural waste with low nutritional properties for animals, constitutes about one fifth of the 500 million metric tons of rice produced annually in the world. Considering that 20% of the grain is husk, and 20% of the husk after combustion is converted into ash, a total of 20 million tons of ash can be obtained. Due to the growing environmental concern, and the need to conserve energy and resources, efforts have been made to burn the husks at controlled temperature and atmosphere, and to utilize the ash so produced as a building material. In the last decades, the use of this residue in civil construction, especially in addition to concrete, has been subject of many researches.

Rice-husk ash (RHA) is a pozzolanic material and its reactivity and particle size depend on the burning and grinding conditions under which it is produced. In general, the average particle size ranges from 5 to 10 μm, and the specific surface area ranges from 20 to 50 m^2/g [1]. The use of RHA as a supplementary cementing material is of great interest to many developing countries where rice production is in abundance. A highly reactive pozzolan is obtained when RHA is burnt under controlled conditions. In other conditions a "residual RHA" is produced with a lower quality, but it can be improved by grinding.

* Corresponding author at: Civil Eng. Department – UNLP, La Plata, Argentina.
E-mail address: zerbino@ing.unlp.edu.ar (R. Zerbino).

http://dx.doi.org/10.1016/j.conbuildmat.2014.08.022
0950-0618/

Zerbino et al. [2] showed that it is possible to use residual RHA "as nature" adopting a mixing process with the coarse aggregates of concrete to reduce the particle size. In that paper results of fresh and mechanical properties as well as water permeability of concretes replacing cement by residual RHA previously grinded (GRHA), RHA without grinding (NRHA) and a Control concrete without ashes were presented. When compared with Control concrete (without ashes) concrete replacing 15% of the cement by NRHA achieved similar mechanical and durability properties. However better results were obtained with GRHA. Regarding other particular properties, it was shown that matrix–aggregate bond strength improved when GRHA or NRHA were incorporated. No significant effects on the stress–strain behavior in compression or in the residual properties after high temperature exposure were found. These results definitively prove that the incorporation of natural RHA in concrete represents a good alternative for disposal of this residue, obtaining some technical benefits, even without the previous optimization through a grinding process, with a significant ecological positive impact.

Nevertheless as RHA contains siliceous vitreous minerals and cristobalite, deleterious reactions, such as alkali–silica reactions (ASR), with portland cement can take place when alkalis and certain environmental conditions are present. Damage due to ASR in concrete was first recognized by Stanton [3] in USA and has since been observed in many other countries. Most researchers agree that is a reaction between certain forms of silica present in the aggregates and the hydroxide ions (OH^-) in the pore solution of the concrete [4]. The three major factors to develop the reaction are: alkalis in the pore solution, reactive silica, present in certain aggregates such as volcanic glass, cryptocrystalline silica (opal, trydimite, cristobalite, and chalcedony), strain quartz and the presence of water. Other factors can play a significant role, such as environmental relative humidity, porosity of the concrete and presence of mineral admixtures. Analytical techniques such as scanning electron microscopy with energy dispersive spectroscopy (SEM/EDS) and/or X-ray diffraction (XRD) together with standard petrographic examination are widely used methodologies in the identification of damaging processes in concrete structures [5].

Microstructural analysis represents a very important tool to evaluate ASR in concrete structures, especially when complemented by macroscopic observations of cracks and other signs of reaction. Microstructural analysis includes examination of plane polished sections, examination of thin sections in a polarization microscope and occasionally scanning electron microscopy (SEM) analysis, as well. The crack patterns are of particular importance in the ASR diagnosis. Many petrographers only use microstructural analyses (i.e. analysis of thin sections and SEM) in their examinations. These analyses give a very good view of details in the interior of a structure, but they are less suited to give a sufficient overview of the extent of cracking in the concrete. The experiences have shown the importance and advantages of using larger samples to describe the crack intensity and crack pattern in drilled concrete cores by analysis of plane polished sections. Thus, a better correlation to what is observed in the field might be obtained. However, the presumption is that an experienced person performs the field survey, in addition to selecting representative sampling locations on the structures. It is also important to carry out a comprehensive visual examination of the drilled cores when they arrive in the laboratory as a basis for detail planning of the laboratory program [6].

Zerbino et al. [7] studied the development of ASR in mortars and concretes prepared with NRHA and GRHA. The experimental work included accelerated and long term expansion tests, mechanical characterization, microscopic observations and studies on prototypes. It was observed that the incorporation of RHA in concrete implies risks of expansions and mechanical degradation by reactions with alkalis. Accelerated tests (ASTM C 1260) in mortars showed that NRHA increases the expansion, while previously ground ash (GRHA) can lead to inhibition or exacerbation of the ASR, depending on the percentage used. It was proved that, as expected, the damage levels strongly depend on the cement used. Thus, when using NRHA the cement must be carefully selected, since some cements can enhance the risk of ASR. It was also observed that the presence of pozzolans can minimize the risk of reaction when NRHA is incorporated. Concretes incorporating GRHA showed expansions (ASTM C 1293) below the limit of 0.040%, while drastic expansions were found in concretes with NRHA. Although the use of NRHA leads to a residual mechanical behavior characteristic of damaged concretes, no typical signs of ASR as the presence of gels were found. Finally, the performance under field conditions of slab prototypes incorporating GRHA and NRHA and different alkalis contents was studied; it was found that when external alkalis were added the degradation of concretes incorporating NRHA was in accordance with the behavior expected from mortar and concrete prisms results. When alkalis were supplied only by the cement, prisms tests and field measurements indicated admitted grades of expansions but a few small fissures were observed on the slab with higher content of cement (Na_2O_{eq} equal to 2.86 kg/m^3).

After four years, cores were extracted from those slabs in order to identify reaction products and to analyze the microstructural characteristics. The objective of this work is to discuss the causes and the damage processes involved in the development of expansions in presence of NRHA. The study is based on optical microscopy observations on thin sections and was complemented with the evaluation of the crack pattern of the slabs and the results of strength and surface strain evolution along the time.

2. Experiences

2.1. Materials

A residual rice husk ash (generated by uncontrolled burning conditions), from Rio Grande do Sul State, Brazil, was used "as nature" without previous grinding. After the burning process, the ash is only dried, homogenised, and packed to ease transport to the laboratory. As explained in a previous paper [2] the weak burnt particles of the natural rice husk ash (NRHA) can be ground during concrete production by adopting an adequate sequence during the mixing process, where the NRHA and the coarse aggregates are mixed together during a certain time before the rest of the component materials are incorporated. As a result, the size of NRHA particles is significantly reduced being the mean size near to 150 μm. Details about the chemical analysis and how the ashes were obtained are presented in [2]. For comparison, an optimized ground rice husk ash (GRHA) obtained by grinding the NRHA for one hour in a ball mill was also used. The Blaine specific surface area of the GRHA was 750 m^2/kg and the particles mean size ranged between 4 and 6 μm, with a few particles as large as 100 μm. Table 1 presents the physical characteristics of the ashes, including size analysis of NRHA after 10 min mixing together with the coarse aggregates in a concrete mixer.

Fig. 1 shows the X-ray diffraction (XRD) analysis of GRHA and NRHA. As expected the results of both ashes are very similar. It can be seen a clear peak of cristobalite (*c*), abundant amorphous siliceous material, evidenced by the elevation of the base line of the diagram between 2θ angles 20° and 30° and some quartz attributed to the presence of impurities.

Fig. 2 shows the results corresponding to the DSC–TGA (differential scanning calorimetry and thermogravimetric analysis). It can be seen in both samples, a total weight loss near to 6% and near 4% when considering from 100 °C. This percentage is attributed to unburned material (see Table 1).

Two Ordinary Portland Cements identified as OPC1 and OPC2 were used; their respective total alkali contents Na_2O_{eq} are 0.66% and 0.80%.

Non-reactive aggregates, siliceous natural sand and granitic crushed stone, were used. The coarse aggregate is a granitic crushed stone 19 mm maximum size that when tested in accordance with ASTM C 1293 gave expansions of 0.006% at 52 weeks. The structures in which it has been used show excellent performance both in strength and durability. The fine aggregate is a siliceous natural sand obtained from the east coast of the La Plata River (fineness modulus 2.36, density 2.63); it has rounded particles composed of quartz (>70%), lithic granitic fragments, feldspars (plagioclase), pyroxenes and a very small amount (0.5%) of chalcedony. Expansion tests according to ASTM C 1293 and ASTM C 1260 indicate expansions of 0.038% at 1 year and 0.080% at 16 days, respectively.

Table 1
Physical properties of RHA.

Identification	NRHA		GRHA
Fineness	Original	After 10 min mixing together with coarse aggregates	Previously grinded in a ball mill
Pass%			
#50	47	81	100
#100	23	39	100
#200	18	15	95
Relative density	1.45–1.60		2.05
Blaine specific surface (m^2/kg)			750
Total weight loss (%)	5.76		6.04
Weight loss from 100 °C (%)	4.01		4.38
Humidity (%)	1.75		1.66

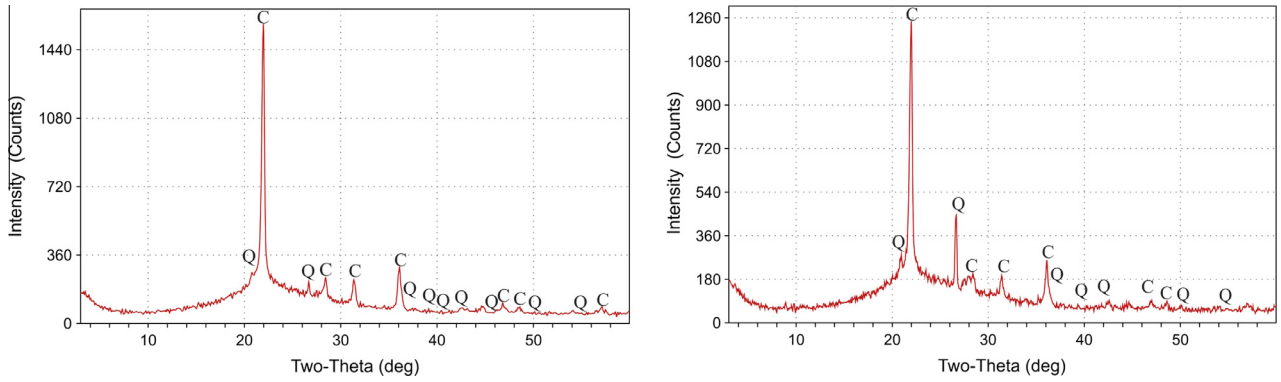

Fig. 1. X-ray diffraction analysis of NRHA (left) and GRHA (right).

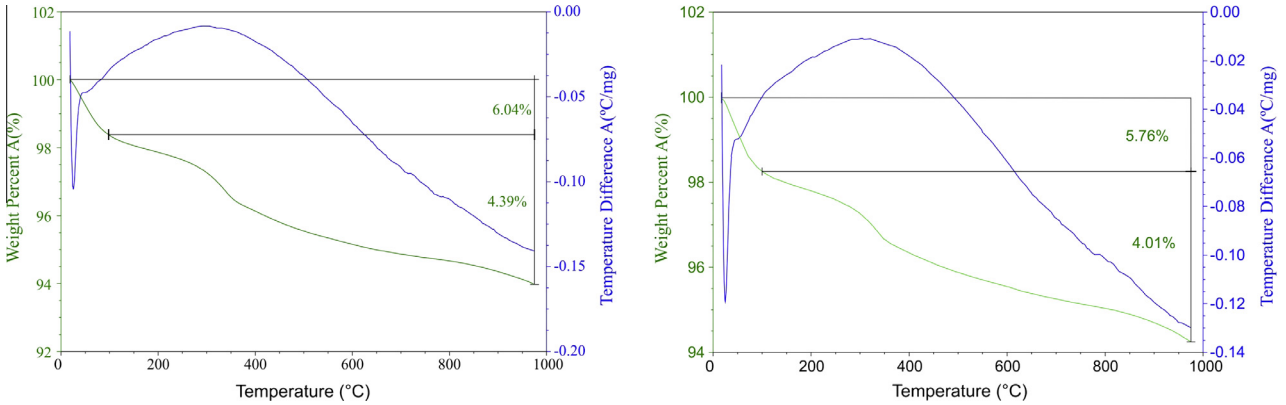

Fig. 2. DSC–TGA analysis of NRHA (left) and GRHA (right).

Regarding the rest of the component materials, potable water and in some cases a high range polycarboxylic based water reduction admixture were used. The superplasticizer was incorporated to compensate the differences in the water demand, especially in the case of NRHA.

2.2. Studies on prototypes

With the aim of evaluating the performance of NRHA in concrete located outdoors, two Series of small slab prototypes were made. They were located within the urban area of La Plata, Buenos Aires Province, Argentina, where the mean meteorological characteristic parameters are temperature 16.6 °C, relative humidity 78% and annual rainfall 1065 mm.

Series A included three 0.80 × 0.60 × 0.20 m slabs prepared with a reference concrete (A1) and two concretes replacing 15% of cement in weight by GRHA (A2) and NRHA (A3). Following the general guidelines of ASTM C1293, NaOH was added to achieve 5.25 kg/m^3 of total alkalis (Na_2O_{eq}). Cement OPC1 was used, having a total cementitious content of 420 kg/m^3.

In addition, 100 × 200 mm cylinders and 75 × 75 × 300 mm prisms were cast. The cylinders were cured for 7 days in a moist room, and then placed by the slabs. The prisms were divided in two sets, one placed by the slabs and the other stored according to ASTM C1293 (38 °C in saturated conditions inside plastic bags). The expansions of the prisms, the length variations on the slab surfaces and the mechanical properties of concretes were measured over the course of three years. Compressive strength and modulus of elasticity were measured following the general guidelines of ASTM C39 and ASTM C469 standards.

As concrete incorporating NRHA showed an important degradation, a second group of prototypes (Series B), including three slabs of 0.50 × 0.50 × 0.10 m, was later studied. In this case all concretes replaced 15% of cement in weight by NRHA, varying the cementitious material and the alkali contents. Cement OPC2 was used. The first concrete (B1) incorporated 5.25 kg/m^3 of total alkalis (Na_2O_{eq}) and 420 kg/m^3 of total cementitious material, the second (B2) used the same binder content but without the addition of alkalis. The third (B3) was also prepared without addition of alkalis, but the total cementitious content was reduced to 330 kg/m^3 (280 kg/m^3 of OPC2 and 50 kg/m^3 of NRHA). With this last mixture proportion, compressive strengths of 30 MPa at 28 days were previously obtained [2].

The slabs were placed in the same conditions as Series A. Prisms and cylinders were cast and the same types of evaluations were performed. Again, the length variations on the slab surfaces and the mechanical properties of the cylinders were measured over the course of near three years. Table 2 summarizes the main characteristics of Series A and B.

Table 2
Characteristics of concretes used in Series A and B.

Concrete	Series A			Series B		
	A1	A2	A3	B1	B2	B3
OPC1 (kg/m^3)	420	357	357			
OPC2 (kg/m^3)				357	357	280
NRHA (kg/m^3)			63	63	63	50
GRHA (kg/m^3)		63				
Na_2O_{eq} (kg/m^3)		5.25		5.25	2.86[a]	2.24[a]
w/c + RHA		0.44		0.44	0.44	0.56
Slump (mm)		180 ± 10			80 ± 5	
Slab dimensions (m)		0.80 × 0.60 × 0.20			0.50 × 0.50 × 0.10	

[a] Supplied by the cement.

2.3. Testing methods

Accelerated expansion tests were performed in accordance with ASTM C1293 using prisms of 75 × 75 × 300 mm, stored at 38 ± 2 °C. The length changes were measured using a mechanical length comparator with a precision of 0.0025 mm. The same measurements were also made on prisms stored by the slabs. In addition, the strains on the surface of the slabs were measured with a mechanical deformation device (0.0025 mm), and a survey of the crack patterns was performed.

The stress–strain behavior under uniaxial compression was evaluated on standard cylinders of 100 × 200 mm. Loading–unloading cycles up to 40% of the maximum stress were applied to determine the modulus of elasticity, after which the load was increased monotonically up to failure. A controlled closed loop system was used, with the axial deformation as the control signal, in order to obtain the complete stress–strain curves.

Petrographics and textural studies on thin sections were carried out. An Olympus B2-UMA trinocular petrographic microscope with a built-in Sony 151A video camera and Image-Pro Plus image processing software were used. A JEOL JSM 35 CP scanning electron microscope, DX4 equipped with energy dispersive X-ray spectrometer (EDS) for semi-quantitative analyses, with an ultrathin window with a range of analysis from $Z = 5$ (B) to $Z = 92$ (U) were used. The samples were covered with a gold film.

For RHA characterization a Rigaku D-Max III X-ray diffractometer set at 35 kV and 15 mA, with Cu Kα radiation (wavelength of 1.54060 Å) and a graphite monochromator in the secondary diffracted beam to remove Cu Kβ radiation were used. Diffractograms from 3° to 60° 2θ, in 0.04° 2θ increments with 1 s counting time per increment were made.

3. Results and discussion

3.1. Macroscopic observations, strength and expansion tests

After only four months concrete A3, replacing 15% of cement in weight by NRHA, presented significant cracking, the cracks in the slab being larger and more numerous than those observed in the cylinders. Fig. 3 shows the appearance of the slabs and the specimens at 4 months. After four years Concretes A1 and A2, reference and with GRHA, remain sound, and no cracking can be appreciated; in the case of concrete A3, severely damaged at early ages, no significant increases in crack pattern were seen.

Fig. 4 compares the evolution of compressive strength and modulus of elasticity measured on standard cylinders and the development of expansion measured on the slabs surfaces and on the different groups of prisms. While in concretes A1 and A2 the compressive strength continuously increases, achieving values higher than 56 MPa at 36 months; concrete A3 shows a decrease in strength between 1 and 4 months and then it gains strength until 3 years, but achieves only 36 MPa. A3 also shows an important decrease in the modulus of elasticity clearly justified by the extensive cracking. The process of damage is reflected in the drastic increases in the expansion of concrete A3, while in A1 and A2 the linear variations are always below the limit of 0.04%.

The mixture proportions of concrete B1 are similar to A3, varying the cement used. Again, drastic expansions, with even higher expansion rate, take place in B1 prepared with 420 kg/m^3 of total cementitious content and 5.25 kg/m^3 of Na_2O_{eq}, with the induction period being strongly reduced in the prisms exposed at 38 °C in saturated conditions (ASTM C 1293). In the prisms and the slabs placed outdoors, the expansions increased up to values higher than 0.2%; with extensive cracking also appearing. The situation differs in B2 and B3 where the alkali contents correspond to those introduced by the cement. The linear length variations were below the limit and, as expected, were smaller in B3, which has the

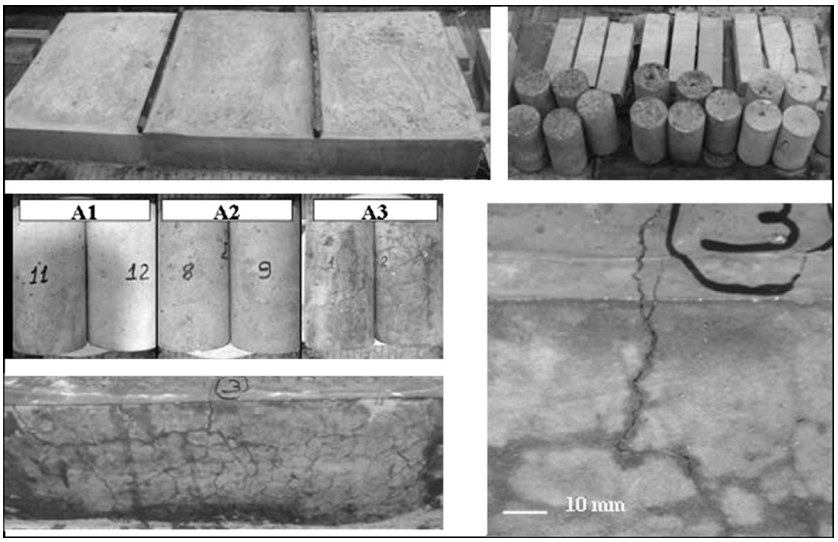

Fig. 3. General view of slabs and specimens of Series A and details of slab A3 at the age of 4 months.

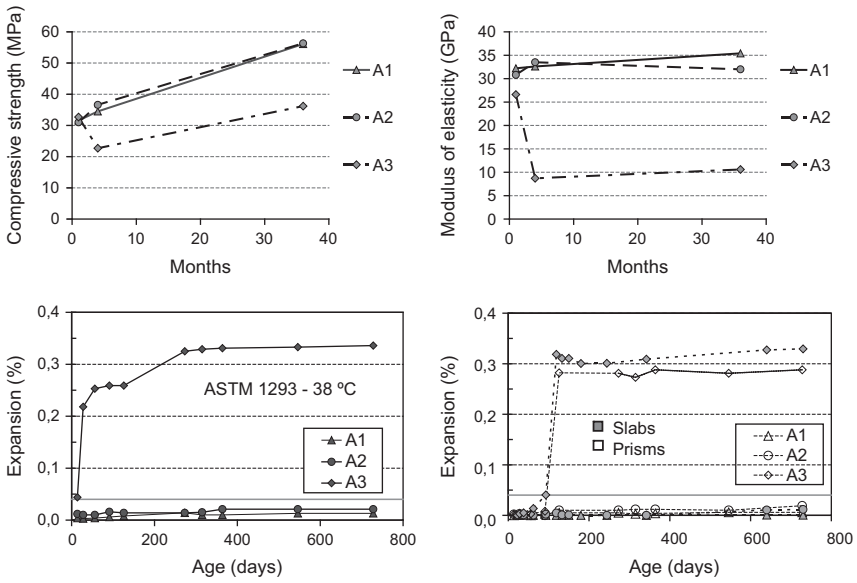

Fig. 4. Series A. Up: evolution of compressive strength and modulus of elasticity. Bottom: evolution of expansions of the slabs surfaces and the different groups of prisms.

lowest total cementitious content. Although the expansions were lower than 0.04%, a few small cracks were seen in the slab cast with B2 at the age of 1 year. After 3 years, concrete B2 shows some increase in expansions (still lower than 0.04%), both measured on the slabs and on the prisms (ASTM C1293). In accordance with this, it was observed an increase in the extent of cracks on the slab

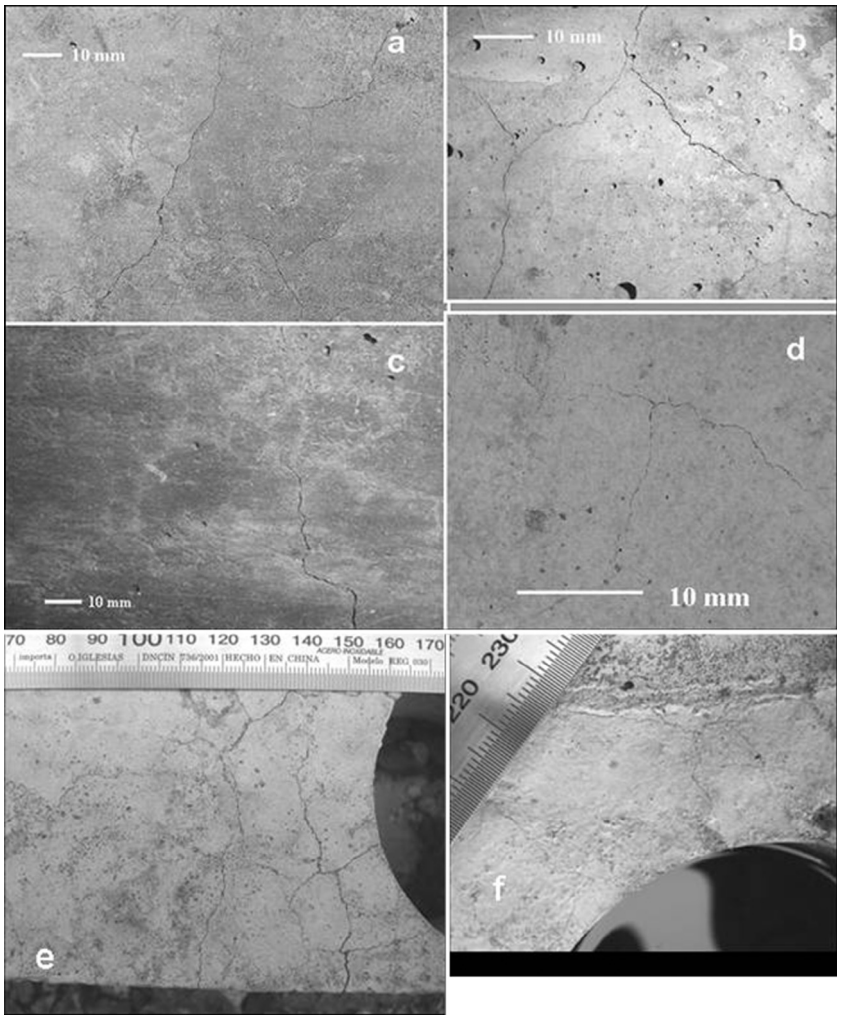

Fig. 5. Series B. View of specimens after 10 months: (a and c) slab B1, (b) cylinder B1, (d) slab B2. View of slabs after 3 years: (e) B1, (f) B2.

surface. However; it must be mention that these are small and thin cracks and that no cracks appeared in the cylinders. Complementarily, the crack widths were measured with a magnifying glass that has a precision equal to 0.05 mm. In B2 the crack width was lower than 0.05 mm, while in B1 and A3 it exceeded 0.30 mm. Fig. 5 shows the aspect of Series B concretes.

Fig. 6 compares the evolution of compressive strength and modulus of elasticity measured on standard cylinders and the

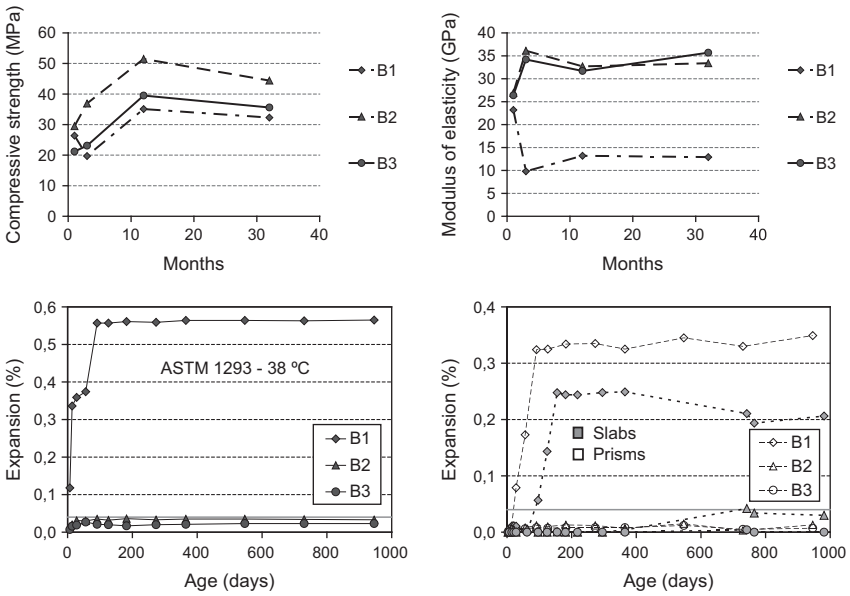

Fig. 6. Series B. Up: evolution of compressive strength and modulus of elasticity. Bottom: evolution of expansions of the slabs surfaces and the different groups of prisms.

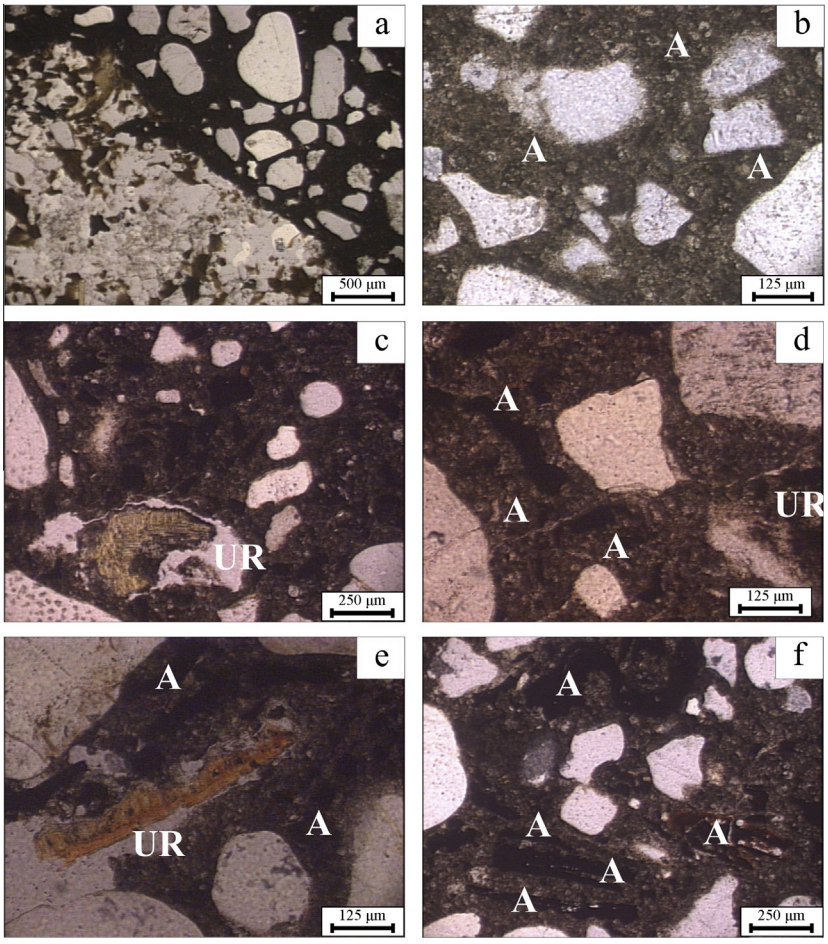

Fig. 7. Optical microscopy observations (with plane-polarized light); A: ash particle, UR: unburned rice husk particle.

development of expansion measured on the slabs surfaces and on the different groups of prisms.

Regarding the mechanical properties it was found that concretes B2 and B3 show evolutions in strength from 1 to 12 months with differences in accordance with the water/binder ratios used. B1 repeats the behavior of A3 and its strength and elastic modulus are lower than in B2, even at 1 month. The strength and especially the stiffness of B1 decrease at 3 months indicating the development of internal damage. After 3 months mechanical properties of B1 were even lower than those of B3. At later ages there is an increase in strength, reflecting the formation of hydration products as in Series A.

3.2. Observations of concretes microstructure

Considering the degradation of the slabs, manifested by the presence of cracks and the decreases in strength and stiffness, it was of interest to explore the internal structure of concrete looking for some reaction products.

Fig. 7 presents some photomicrographs corresponding to the observations made with optical microscopy on cores obtained from each concrete slab. Fig. 7a–c shows, at the age of 4 years, the aspect of Series A; Fig. 7d–f correspond to Series B and were obtained at 3 years.

In reference concrete (A1, without RHA incorporating 5.25 kg/m^3 of alkalis and 420 kg/m^3 ordinary portland cement) no microcracks are seen and the interfaces between the coarse or fine aggregates and the cement paste are good and there are no signs of reaction in this sample. Fig. 7a shows a view with parallel light.

In concrete A2 (prepared with GRHA, 5.25 kg/m^3 alkalis and 420 kg/m^3 total binder material content) the paste appears sound and without microcracking or reaction signs; the ash particles (A) are very small and they are homogeneously distributed inside the cement paste. Fig. 7b shows a detail obtained with parallel light of a sector of this mortar.

In the case of concrete A3 which incorporates NRHA, 5.25 kg/m^3 of alkalis and 420 kg/m^3 total binder material content, significant microcracking is present near the coarse aggregate and inside the

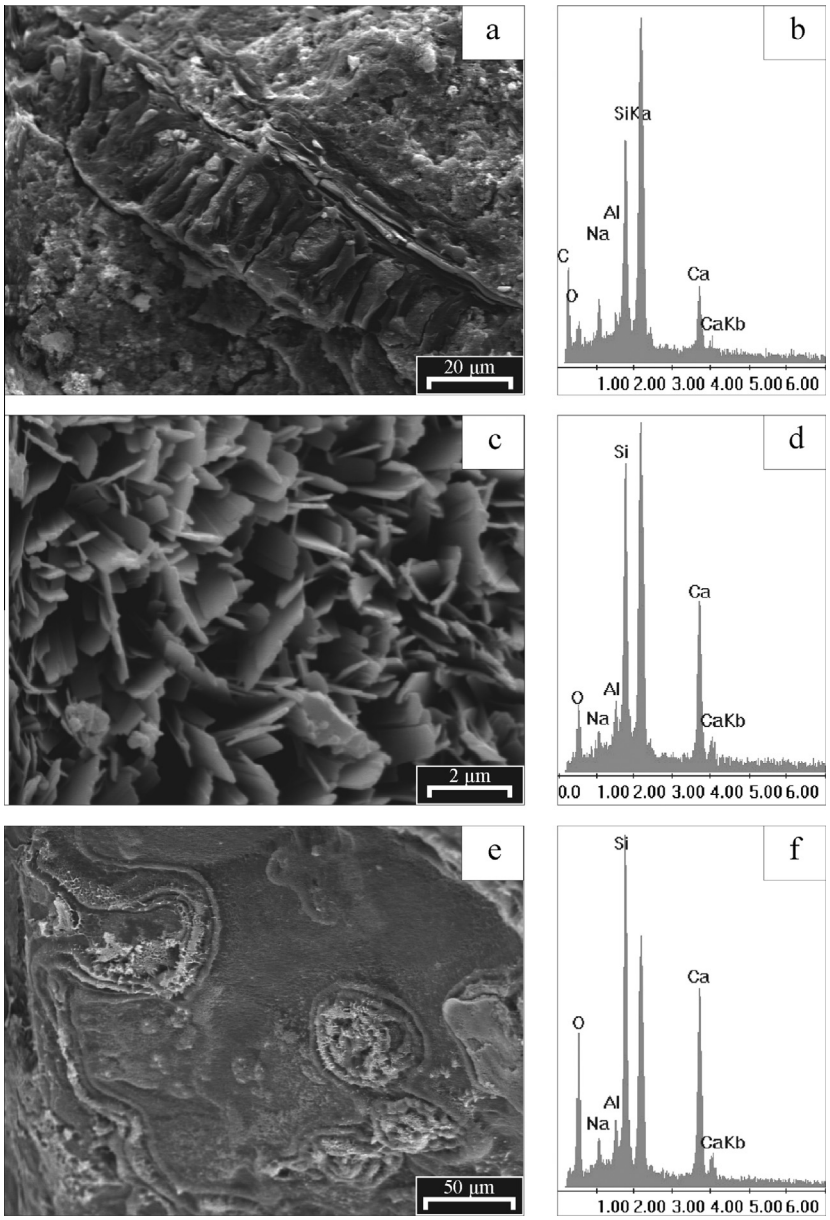

Fig. 8. SEM–EDS observations.

Table 3
Signs of deterioration observed in concretes that can be associated to ASR.

Concrete	Series A			Series B		
	A1	A2	A3	B1	B2	B3
Expansion	N	N	H	H	L	L
Loss of compressive strength	N	N	M	M	L	L
Loss of stiffness	N	N	H	H	L	L
Presence of gel	N	N	N	N	N	N
Cracks and voids close to unburned rice husk particles	N	N	H	H	L	N
Cracks at the mortar–aggregate interfaces	N	N	L	L	N	N

N: none; L: low; M: medium; H: high.

cement paste. Paste cracking generally appears associated to unburned rice husk particles; while observed at the microscope using crossed nicols they are birefringent (indicating that they are anisotropic; thus they are not amorphous and therefore that they have not been completely burnt).

Fig. 7c shows an unburned rice husk particle (UR) associated to microcracks together with abundant husk ashes. In this concrete there are abundant microcracks and many of them cut the ashes. It was also observed the presence of unburned rice husk particles close to big voids that can be related with some shrinkage process.

Concrete B1 shows similar characteristics as A3, with multiple cracking associated to the presence of unburned rice husk particles (see Fig. 7d).

The sample of concrete B2 (incorporating NRHA, 2.86 kg/m^3 of alkalis and 420 kg/m^3 total binder material content) shows rice husk ash (A) together with unburned particles (UR) with anisotropic characteristics (Fig. 7e). In this case the interface contacts are well defined and no cracks are observed inside the cement paste; only in one sector a microcrack associated to an unburned husk was observed.

Finally, the sample of concrete B3 (with NRHA, 2.24 kg/m^3 of alkalis and only 330 kg/m^3 total binder material content) looks in very good conditions. Cracks or other signs of reaction are not present; in addition, the coarse aggregate–mortar interfaces are well defined and only isotropic particles are present. Fig. 7f shows ash particles (A) inside a sector of mortar without damage.

It is important to note that, although it is evident that the reaction takes place with the NRHA in presence of alkalis, no gel was found inside the structure of any of the damaged concretes.

With the aim of evaluating the morphological characteristics of the RHA particles as well as their chemical composition, SEM–EDS observations were performed in A3. Fig. 8a shows a particle of RHA, it can be seen the structure of the biological material and at the periphery the formation of a platy layered material. The EDS of Fig. 8b shows the presence of C together with Si, Na, Ca and Al. Fig. 8c shows the morphological characteristics of the neoformation material developed inside a void; Si and Ca and traces of Al and Na are present in the chemical composition (Fig. 8d). Finally, Fig. 8e shows the development of neoformation products on the surface of an aggregate particle. The chemical composition is similar to that found inside the voids and other portions of the concrete (Fig. 8f).

Table 3 shows the main signs of deterioration observed in the different concretes that can be associated to ASR.

Summarizing, concretes incorporating NRHA with high alkali content (A3 and B1), presented significant damage at ages as low as 3 or 4 months, with important reductions in strength and stiffness and extensive cracking in cylinders and slabs. At later ages there were not important increases in the expansions or in the level of damage, showing some evolution of strength attributed to the cement hydration and pozzolanic reactions of RHA. No gel or other typical signs of ASR were found in these concretes at any age.

Concretes with high alkali content, but with GRHA or without RHA (A2 and A3), remain undamaged after 4 years, and with strength levels over 50 MPa.

Concrete B3 with NRHA and low alkali content (lowest cement content) after 3 years does not show expansions or cracks; however there is a light decrease in strength. Finally, concrete incorporating NRHA with high cement content (intermediate alkali content) showed strength gains up to one year and at 3 years there were losses of strength. At 1 year it presented few small cracks and at 3 years new cracks appear, however they remain very small.

4. Conclusions

The study of slabs prepared with concretes incorporating natural rice husk ash and high alkalis contents, exposed over three years outdoors, shows that:

- Visual and microscope observations performed in concretes incorporating NRHA, when there is high alkali availability (concretes B1 and A3 incorporating Na_2O_{eq}: 5.25 kg/m^3) and the temperature and humidity conditions are proper for the development of ASR, show clear signs of damage produced by the development of expansive reactions. Although not gel was found, there were observed numerous cracks and voids close to unburned rice husk particles. In addition, some cracks at the mortar–aggregate interfaces were found. High expansions and significant decreases in strength and stiffness were measured, since early ages.
- In concretes with lower alkalis contents (Concrete B2: Na_2O_{eq}: 2.86 kg/m^3, Concrete B3: Na_2O_{eq}: 2.24 kg/m^3), even with the same percentages of NRHA, the expansions were lower than 0.04% and there were no significant decreases in the mechanical properties. In this case, no extensive cracking and a clear contact at the mortar–aggregate interfaces were observed. The situation is obviously better in concrete B3 where only 330 kg/m^3 total binder material content was used. After 3 years there was no significant degradation in these cases, only few and small cracks were observed on the slab with the highest content of cement (B2).
- In concrete A2, incorporating Na_2O_{eq}: 5.25 kg/m^3 and GRHA, the microscope observations show a much finer RHA along a compact matrix where no cracks appear. In this case, the mechanical properties improved with time. As expected no damage was observed in the reference concrete (A1) without RHA.

Acknowledgments

This work was initiated with the support of the Programa Sul-Americano de Apoio às Atividades de Cooperação em Ciência e Tecnologia PROSUL-CNPq (South-American Support Program to Cooperation Activities in Science and Technology) to the project "Production of structural concrete with natural rice husk ash with-

out optimization" developed under the general coordination of Prof. G.C. Isaia (Universidad Federal de Santa Maria, RS, Brazil) and the participation of Eng. O.R. Batic and the collaboration of Eng. D. Falcone. The authors also wish to thank the LEMIT, the CIC from the Province of Buenos Aires, CONICET and the Geology Department of the Universidad Nacional del Sur for their helpful support during the research.

References

[1] Zhang MH, Lastra R, Malhotra VM. Rice-husk ash paste and concrete: some aspects of hydration and the microstructure of the interfacial zone between the aggregate and paste. Cem Concr Res 1996;26(6):963–77.

[2] Zerbino R, Giaccio G, Isaia GC. Concrete incorporating rice husk ash without processing. Constr Build Mater 2011;25(1):371–8.

[3] Stanton T. Expansion of concrete through reaction between cement and aggregate. Proc Am Soc Civ Eng 1940;66(10):1781–811.

[4] Ferraris CF. Alkali–silica reaction and high performance concrete. In: Building and fire research laboratory. Gaithersburg, MD 20899: National Institute of Standards and Technology; 1995. 24 p.

[5] Rivard P, Fournier B, Ballivy G. The damage rating index method for ASR affected concrete – a critical review of petrographic features of deterioration and evaluation criteria. Cem Concr Aggr 2002;24(2):81–91.

[6] Lindgård J, Haugen M, Castro N, Thomas MDA. Advantages of using plane polished section analysis as part of microstructural analyses to describe internal cracking due to alkali–silica reactions. In: Proc. 14th international conference on alkali-aggregate reactions (ICAAR). Austin, Texas (USA); 2012. 10 p.

[7] Zerbino R, Giaccio G, Isaia GC. Alkali–silica reaction in mortars and concretes incorporating natural rice husk ash. Constr Build Mater 2012;36:796–806.